Energy & Environmental Science

Accepted Manuscript

ROYAL SOCIETY OF CHEMISTRY

www.rsc.org/ees

Journal Name

COMMUNICATION

A novel cross-linked nano-coating for carbon dioxide capture

Qiang. Fu,‡[ab] Jinguk. Kim,‡[ab] Paul. A. Gurr,[ab] Joel. M. P. Scofield,[ab] Sandra. E. Kentish[a] and Greg. G. Qiao[ab]

Received 00th January 20xx,
Accepted 00th January 20xx

DOI: 10.1039/x0xx00000x

www.rsc.org/

Ultra-thin (~ 100 nm) films with uniform thicknesses can facilitate high CO_2 permeation and are of potential technological significance for CO_2 capture. Among many approaches for obtaining such materials, the recently developed continuous assembly of polymers (CAP) technology provides a robust process, allowing for the production of defect-free, cross-linked and surface-confined thin films with nanometer scale precision. Through utilization of this nanotechnology, we have constructed composite membranes containing cross-linked ultra-thin surface films. The membrane materials formed exhibited significantly high permeances as well as excellent gas separation selectivity.

Membrane technology is considered a promising and environmentally friendly alternative for the mitigation of anthropological CO_2 emissions, due to its adaptability and low energy consumption in comparison with conventional methods when separating CO_2 from a mixed gas stream.[1,2] Previously, gas permeability, a parameter which is based on the gas flux per unit film thickness, was considered the key characteristic for measuring gas separation performance.[3-5] However, in a more practical sense, increased gas permeance, which is a measure of the absolute gas flux through a membrane, without the loss of selectivity, has been recognised as a more important consideration in achieving a competitive membrane process for CO_2 separation in real industrial applications.[6,7] Using the latter measurements, traditional polymeric membranes have shown insufficient capability for CO_2 removal due to their overall low permeance (flux) of CO_2 regardless of their permeability.[1,4] Recently developed ultra-thin film composite (UFC) membranes consisting of a thin polymeric selective layer (~ 100 nm) and a highly porous substrate show the potential to overcome the limitations of low gas flux, since the ultra-thin top layer can minimize gas trans-membrane resistance and thus maximize gas flux while retaining selectivity.[7] In addition, composite membranes have the added advantages of reduced fabrication costs. The key challenge is to produce a gas separation layer with a sub 100 nm thickness which can exhibit a robust performance. At present, flat sheet composite membranes are typically produced by slot die coating or using doctor blades,[8] while dual layer hollow fibres are constructed using co-extrusion.[9,10] These methods are all based on the physical addition of polymers in forming a membrane which can readily be dissolved due to the lack of covalent attachment to the

Broader context

The release of large quantities of CO_2 into the atmosphere has been linked to global warming and climate anomalies. Membrane separation offers a potentially viable energy-saving alternative for CO_2 capture in comparison with conventional technologies, such as amine absorption. However, currently available gas separation membranes do not have sufficiently high permeances (flux) for large scale application which require the treatment of high volume post combustion flue gases containing a CO_2 concentration of 10-15 vol. %. Ultra-thin (~ 100 nm) films with uniform thicknesses can facilitate high CO_2 permeation and are of potential technological significance for CO_2 capture. Utilizing the recently developed continuous assembly of polymers (CAP) technology, defect-free, cross-linked and surface-confined thin films with nanometer scale precision, suitable for CO_2 capture, have been prepared. A significant advantage over existing membranes in this field is that they simultaneously crosslink during the film formation and can be readily fabricated using existing production facilities. Therefore, this nano-coating technology has the potential for the treatment of large gas streams, and particularly for the separation of CO_2 from natural gases or the flue gas generated by coal fired power stations.

[a] *Cooperative Research Centre for Greenhouse Gas Technologies, The University of Melbourne, Parkville, VIC 3010, Australia.*
[b] *Polymer Science Group, Department of Chemical and Biomolecular Engineering, The University of Melbourne, Parkville, VIC 3010, Australia. E-mail: gregghq@unimelb.edu.au*

† Electronic Supplementary Information (ESI) available: [details of the synthesis of polymer precursors and the fabrication of ultra-thin film composite membranes]. See DOI: 10.1039/x0xx00000x

‡ There authors contribute equally.

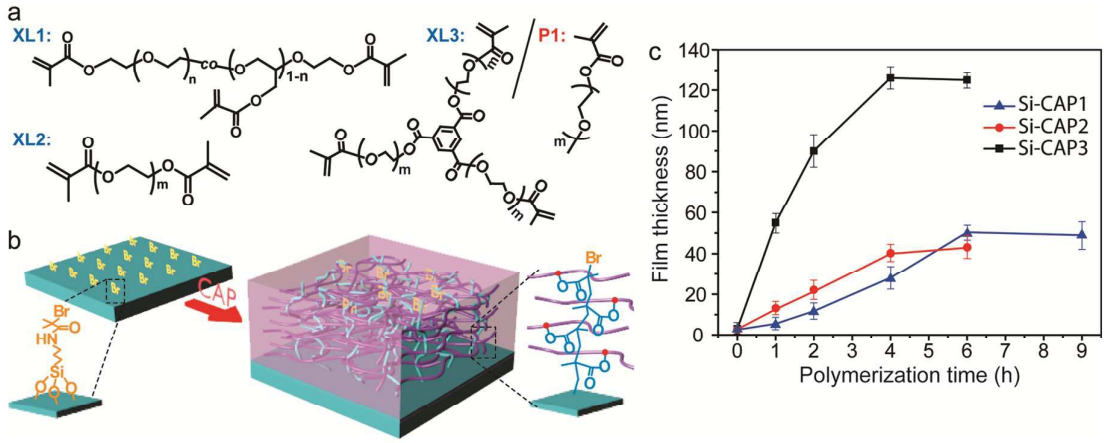

Fig. 1 (a) Chemical structures of the macrocross-linkers (XL1-XL3) and monofunctional polymer precursor P1. (b) Schematic illustration of CAP at the present of $CuBr_2$/Me_6TREN/Na-ascorbate/XLs to afford the ultra-thin films. (c) Thickness growth profile of CAP films (namely Si-CAP1-3) as a function of the polymerization time from a model experiment on silicon wafer, obtained by AFM.

surfaces. Therefore problems associated with such composite membranes include weak mechanical strength, uneven thickness cover, delamination and pinhole defects,[8] which have often resulted in unsatisfactory performance. Therefore, it currently remains an ambitious challenge to develop UFC membranes with tunable nanoscale thicknesses which are chemically and mechanically robust and have desirable selectivity for CO_2 gas separation.

We have recently developed a continuous assembly of polymers (CAP) nanotechnology combining the compositional flexibility of a grafting-to approach, with the direct cross-linking capability of a grafting-from approach.[11-15] Ultra-thin films produced by CAP are chemically bonded to the surface of the substrate, cross-linked throughout the film and have thicknesses ranging from 40 to 140 nanometers. We see this as an opportunity to fabricate tailored nano-engineered composite membranes utilizing CAP techniques[12] with high CO_2 gas permeances. An immediate challenge in developing this membrane material is designing an economical macrocross-linker, a key precursor for the CAP process, which provides for a high CO_2/N_2 selectivity. We also considered that to achieve very high CO_2/N_2 selectivity, the cross-linker must have favourable interactions with CO_2 to enhance solubility selectivity as well as polymerizable functionalities. Guided by these material design principles, we prepared a family of macro-crosslinkers based on polyethylene glycol (PEG). Despite the facts that PEG-based separation membranes may have weak mechanical strength and a strong tendency to crystallize,[16] the CAP process crosslinks the PEG precursors as they form top layer of UFC membranes, simultaneously suppressing any crystallinity as well as enhancing the membrane's mechanical strength.

Herein, we report a new and novel composite membrane using CAP technology to fabricate defect-free ultra-thin separation layers *via* atom transfer radical polymerization (ATRP)[17-19] of PEG-based macrocross-linkers on top of a highly permeable polydimethylsiloxane (PDMS) initiator layer, which is precoated onto a microporous polyacrylonitrile (PAN) substrate. The ability of such membranes to selectively separate CO_2 from N_2 was tested utilizing a constant pressure variable volume (CPVV) apparatus. The CAP UFC membranes displayed an unusually high CO_2 permeance with a high CO_2/N_2 selectivity. Additionally, the CAP ultra-thin separation layer alone exhibits an even higher CO_2 permeance, providing the true potential of this technology specifically towards an efficient and economically viable CO_2 capture process.

In this study, both synthesized and commercially available PEG derivatives (Fig. 1a) were employed in the ATRP-mediated CAP process. Specifically, the macrocross-linker XL1 (M_n = 20 kDa) with over 40 pendant methacrylate groups per chain and the XL3 (M_n = 1.5 kDa) with three pedant methacrylates were specially synthesized (Fig. S1-S3, ESI†). The XL2 with di-functional methacrylate groups (M_n ~ 570 Da) and poly(ethylene glycol) methyl ether methacrylate (P1, M_n ~ 500 Da) which acts as a spacer in the copolymerization with XL3, are commercial products. Firstly, a kinetic study of the growth of the ultra-thin film on silicon wafers was investigated (Fig. 1b). Initially, 3-(2-bromoisobutyramido) propyltriethoxysilane (BIBAPTES, Fig. S4, ESI†) was immobilized onto silicon wafers as the initiator for the ATRP-mediated CAP process. The kinetic study of film growth was conducted by immersing these substrates into an aqueous solution containing $CuBr_2$/Me_6TREN, sodium ascorbate and the PEG macrocross-linkers *via* ARGET-ATRP.[18] Samples were taken at different time intervals, soaked in purified water, dried *in vacuo* and measured for formed CAP film thicknesses. The CAP film thicknesses as analysed by an AFM scratch analysis method are presented in Fig. 1c. The thickness of the CAP film formed using cross-linker XL1 (namely Si-CAP1), increased from 12 nm (after 2 hrs polymerization) to 50 nm after 6 hrs polymerization (Fig. S5, ESI†). Based on the slope of the kinetic plot, the film growth rate for Si-CAP1 and Si-CAP2 after initial polymerization was almost the same, followed by a plateauing of the film thickness after 6 or 4 hrs for Si-CAP1 or 2, respectively. Within experimental error the film thicknesses for Si-CAP1 and Si-

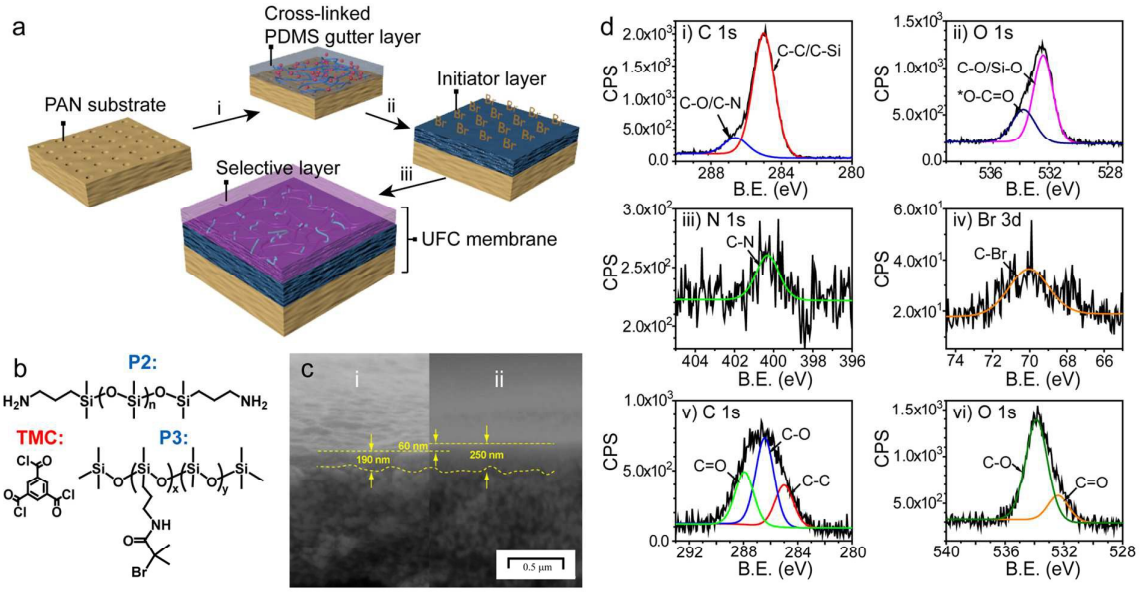

Fig. 2 (a) Schematic illustration of the UFC membrane formation: i spin-coating of P2/TMC to prepare the PDMS gutter layer; ii spin-coating of P3/TMC to prepare of the initiator layer; iii CAP in the presence of $CuBr_2$/Me_6TREN/Na-ascorbate/cross-linkers (XLs) to afford the UFC membranes. (b) Chemical structures of the 1,3,5-Benzenetricarbonyl trichloride (TMC), polymer precursors aminopropyl terminated polydimethylsiloxane P2 and the bromo-functionalized PDMS macroinitiator, poly(DMS-co-BIBAPMS) P3. (c) SEM microphotographs of the cross section of i the PDMS initiator layer and ii the UFC membranes (UFC1-6h in Table S1, ESI†). The interface between CAP film and intermediate PDMS layer cannot be distinguished, but by superimposing images of the PDMS initiator layer and multilayer UFC membranes, the thickness of the top layer can be estimated, ~60 nm. The scale bar represents 500 nm. (d) High resolution XPS spectra of i C 1s, ii O 1s, iii N 1s, iv Br 3d for the PDMS initiator layer and of v C 1s, vi O 1s for UFC membranes (UFC1-6h).

CAP2 are identical. The growth rate in film thickness for Si-CAP3 by copolymerizing XL3 and P1 (XL3:P1 ~ 1:3 wt. %) is substantially faster and leads to a film twice as thick as the other cases. This effect is due to be the addition of the monofunctional P1 acting as a spacer in the film forming process resulting in an increase in the final film thickness. The cessation of film growth is predominately due to the 'burial' of the propagating species within the growing polymer layers and/or catalyst deactivation.[12,13] Therefore, these results reveals the polymerization characteristic of the selected PEG macrocross-linkers in the ultra-thin film formation process.

A general approach to fabricate UFC membranes *via* CAP technology is illustrated in Fig. 2a. A PAN microporous substrate is employed as the support layer of the UFC membranes, to offer sufficient mechanical strength. A solution of amino-terminated PDMS (P2) and 1,3,5-benzenetricarbonyl trichloride (TMC) is spin-coated onto the PAN substrate to afford a highly permeable cross-linked PDMS gutter layer (Fig. 2a-i), followed by introducing a bromo-functionalized PDMS precursor (P3, Fig. 2b, Fig. S6 and S7, ESI†) as the initiator layer for the subsequent CAP process (Fig. 2a-ii). Thereafter, the CAP of PEG macrocross-linkers (XL1, XL2, XL3/P1) was achieved by utilizing well-established ATRP[19] in aqueous solution. The single-step CAP process, *via* propagating radical species transferred through the CAP film, results in UFC membranes with surface-confined and cross-linked ultra-thin top layers (Fig. 2a-iii).

Specifically, the PDMS gutter layer is pre-coated onto the PAN substrates, acting as a protective coating, which prevents the penetration of dilute polymer solution into the porous structure rendering the entire membrane surface smooth.[20] Subsequent coating of PDMS-based macro-initiator P3, affords the PDMS initiator layer, which provides sufficient initiation sites for the following ATRP of PEG macrocross-linkers. Scanning Electron Microscopy (SEM) analysis was carried out on a number of different samples to determine the thickness of the PDMS gutter and initiator layers (Fig. S8, ESI†). The SEM image of a representative initiator layer is shown in Fig. 2c-i, with a PDMS coating thickness of 190 ± 20 nm. Additionally, Attenuated Total Reflectance Fourier Transform Infrared (ATR-FTIR) spectroscopy (Fig. S9a, ESI†) and X-ray Photoelectron Spectroscopy (XPS, Fig. S10a-i, ESI†) were used to confirm the preparation of the PDMS initiator layer. The deconvoluted C 1s, O 1s, N 1s and Br 3d spectra (Fig. 2d i-iv), provide evidence of surface confined functional groups present on the initiator layer. AFM analysis also verified the addition of the PDMS initiator layer, which led to an improvement in the surface roughness from ~32 nm for the untreated PAN substrate, to ~3.9 nm after treatment (Fig. S11a-b, ESI†). The gas separation performance of the PDMS initiator layer was determined by the CPVV apparatus (Fig. S12a, ESI†). The average CO_2 permeance reached 2,800 ± 100 GPU (1 GPU = 10^{-6} cm^3(STP) cm^{-2} s^{-1} $cmHg^{-1}$) with a CO_2/N_2 selectivity of approximately 10, which is in agreement with previously reported work[10] and demonstrates the successful formation of a PDMS gutter layer without any leakage.

The single-step fabrication of the PEG-based cross-linked selective layer on top of the gutter layer, was performed by immersing the P3 coated substrates into aqueous solutions containing different macrocross-linkers (XL1, XL2 or XL3/P1). Different polymerization times produced a range of UFC membranes, named as UFC*x*-*y*h, (Table S1, ESI†), where *x* and *y* indicate the macrocross-linker used and the polymerization time, respectively. The cross-sectional morphology of the UFC membrane observed by SEM analysis is illustrated in Fig. 2c-ii and Fig. S8 (ESI†). The thickness of the CAP selective layers were calculated by subtracting the thickness of the initiator layer, leading to estimated values of ~ 60, 45 and 125 nm for UFC1-6h, UFC2-4h and UFC3-4h, respectively. These observations are in good agreement with the AFM analysis. The CAP-UFC membrane formation was confirmed by the ATR-FTIR (Fig. S9b-d, ESI†) and XPS analysis (Fig. 2d v-vi and Fig. S10b-iv and vi, ESI†). The strong bond at 1728 cm^{-1} assigned to C=O stretching vibration is a feature of saturated esters of PEG-based XLs. The C 1s and O 1s signals also have been altered after the growth of the ultra-thin film. For example, the deconvoluted C 1s spectrum signal at 288.0 eV is attributed to the carbons in the carbonyl bond associated with the methacrylate moieties of XL1. Due to the controlled nature of the CAP process, the surface roughness of the resultant CAP UFC membranes was even smoother, with UFC2-4h, for example having a RMS of ~3.0 nm (Fig. S11c, ESI†).

The ability of these UFC membranes to selectively separate CO_2 from N_2 was then tested utilizing a CPVV apparatus (Fig. S12a, ESI†) at a temperature of 35 °C and a feed pressure of 340 kPa (gauge pressure). A minimum of three UFC membranes per macrocross-linker were prepared with good reproducibility; the variation of membrane permeation performance is within 14 % for all membranes. Fig. 3a-c shows the dependence of CO_2 single gas permeation and CO_2/N_2 selectivity on the polymerization time. In all cases, CO_2 permeance of these UFC membranes decreased, while CO_2/N_2 selectivity increased when extending the polymerization time, reflecting the formation of a thicker film. Defect-free CAP-UFC membranes formed over 6h polymerization for XL1 or 4h polymerization for XL2 or XL3/P3, showed excellent CO_2 permeance

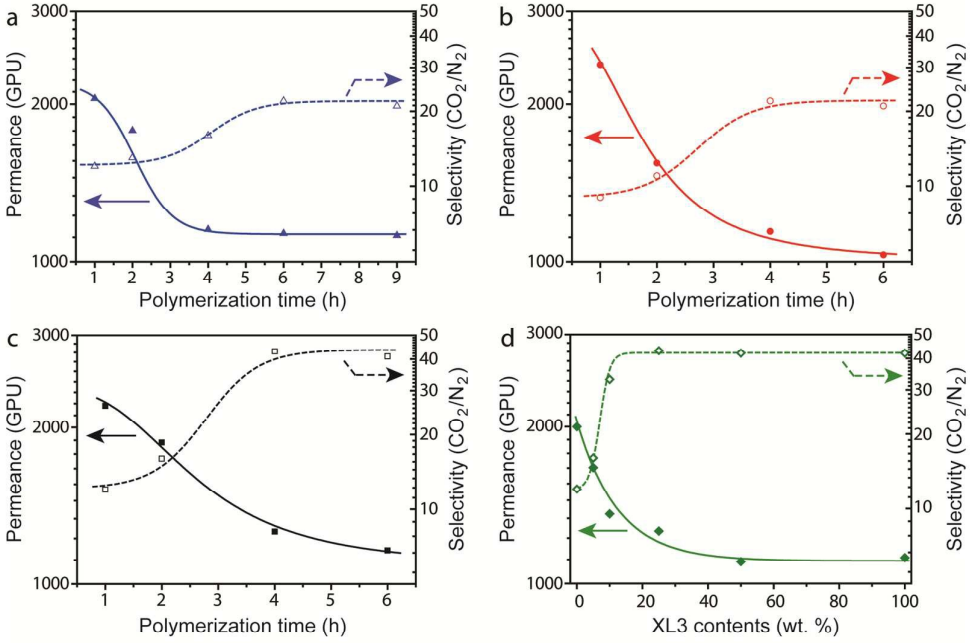

e

Composite Membranes	Single gas permeation			Mixed gas permeation		
	J_{CO_2} (GPU)	J_{N_2} (GPU)	α (CO_2/N_2)	J_{CO_2} (GPU)	J_{N_2} (GPU)	α (CO_2/N_2)
Initiator layer	2,880	290	10	1,820	260	7
UFC1-6h	1,130	51	22	1,090	99	11
UFC2-4h	1,140	52	22	1,100	100	11
UFC3-4h	1,260	32	43	1,210	56	22

Fig. 3 (a-c) CO_2 permeance (solid symbols) and CO_2/N_2 selectivity (empty symbols) through UFC1, 2 and 3 series membranes as a function of polymerization time via single gas test, respectively. (d) CO_2 permeance (solid symbols) and CO_2/N_2 selectivity (empty symbols) through UFC3 series membranes as a function of XL3 contents. (e) The comparison of CO_2 permeance and CO_2/N_2 selectivity through the PDMS initiator layer, UFC1-6h, UFC2-4h and UFC3-4h membranes under single and mixed gases (CO_2/N_2 = 30/70 mol.%) permeation conditions.

of > 1,100 GPU and good CO_2/N_2 selectivities between 20-40.

The separation of gas pairs in polymeric membranes is defined by the selectivity, $\alpha_{A/B}$, which in turn is dependent upon the relative solubility and diffusivity of the components.[21] Recent studies have demonstrated that end functionalities, side chain grafting and cross-linking could affect the gas transport properties in PEG-based membranes.[22-24] Therefore, we designed a series of UFC membranes by copolymerizing different composition ratios of 3-arm-PEG (XL3) and PEG methyl ether methacrylate (P1), namely UFC4-*x*% (Table S2, ESI†). XL3 contains EG units in its backbone separated by an aromatic spacer, while P1 has grafting EG units. The gas separation performance of this series of UFC membranes as a function of XL3 mass loading are shown in Fig. 3d. Decreasing XL3 content leads to an increase in CO_2 solubility and a decrease in cross-linking density of the selective layer, which ultimately results in pinhole defects at XL3 < 10 *wt.*%. Inspection of the data (Table S2, ESI†) reveals that both the CO_2 permeance and CO_2/N_2 selectivity remains constant (1,100 - 1,300 GPU and α (CO_2/N_2) > 40) when the XL3 mass loading is above 25 *wt.*%; below which point the CO_2 permeance increases (from 1,260 to 2,000 GPU) but the CO_2/N_2 selectivity sharply decreases to 12 when further decreasing XL3 content to 0 *wt.*%.

Mixed gas permeation experiments were subsequently carried out using the setup is shown in Fig. S12b (ESI†) and its operation described elsewhere.[25] The experiments were conducted with a feed mixture of 30/70 mol. % for CO_2/N_2 at 35 °C. We first studied the effects of stirrer speed on CO_2 permeance measurements (Fig. S13, ESI†). The minimum stirrer speeds were determined to be 500 rpm for feed side and 300 rpm for permeate side to ensure the effect of concentration polarization was eliminated. In all cases, gas behavior typical of rubbery-like membranes was observed. When comparing mixed gas and single gas measurements, the CO_2 flux is unaffected, however the selectivity is reduced for mixed gas analysis (Fig. 3e and Table S1, ESI†). For example, in case of UFC2-4h the CO_2/N_2 selectivity decreased from 22 to 11, and the CO_2 permeance is only slightly reduced (1,100 GPU) between single and mixed gas analysis. This behavior is typically a result of CO_2 induced plasticization, which results in an increase in nitrogen permeance relative to the single gas case. A similar phenomenon has been observed previously in CO_2/light gas separation (*i.e.* CH_4 and N_2) in PDMS[10] and PEG[26] based membranes.

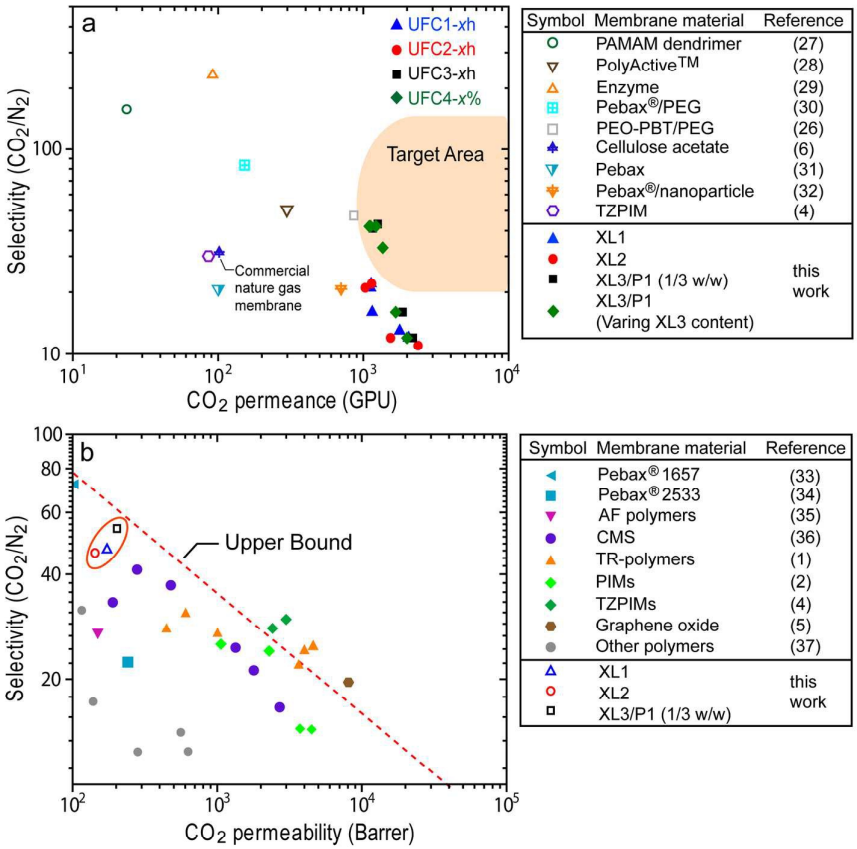

Fig. 4 (a) CO_2/N_2 selectivity versus CO_2 permeance plot comparing the performance of UFC membranes with membranes reported in the literature 26-32. The target area is that proposed by Merkel *et al.* from ref. 6 for post combustion capture of CO_2. (b) The relationship between CO_2 permeability and CO_2/N_2 selectivity of UFC1-6h, UFC2-4h and UFC3-4h selective layers compared to other membranes reported in the literature 33-37. Measurements are for single gases and the 2008 upper bound is from ref. 3.

Fig. 4a shows the comparison of UFC membranes presented in this study with polymeric membranes for CO_2/N_2 separation, demonstrating the superior performance of the UFC membranes. The target area for post combustion capture, proposed by Merkel *et al.*,[6] based on the economics of gas separation is also included in the plot for comparison. Membranes require high CO_2 permeance (≥ 1000 GPU) and modest selectivity (≥ 20) to reach this target performance area. Membranes with lower CO_2 permeance will require a larger membrane area, while membranes with a selectivity of less than 20 are unlikely to be selective enough, resulting in larger capture cost regardless of their permeance. In addition, membranes with a selectivity of much more than 100 are likely to be too selective and require too large a membrane area due to pressure-ratio-issues.[6] In comparison with conventional cellulose acetate membranes, the UFC1-6h and UFC2-4h present a much higher CO_2 permeance of > 1,100 GPU with medium CO_2/N_2 selectivity of ~ 20. Furthermore, the UFC3-4h showed higher CO_2 permeance of ~ 1,300 GPU as well as excellent CO_2/N_2 selectivity of 43, which is in turn, ten times more permeable than conventional cellulose acetate membranes (110 GPU).[6] As apparent from Fig. 4a, the gas separation performance of these CAP-UFC membranes (UFC3-4h and 6h and UFC4-10% to 100%) fell within the target performance area. Additionally, the selective layers alone displayed much higher CO_2 permeance of ~ 3,000 GPU with CO_2/N_2 selectivity of 40-60 (unfilled symbols, Fig. S14, ESI†). The lower permeance of the UFC3-4h selective layer (unfilled square) results from its relatively thicker selective layer (~ 125 nm), which is almost double that of the UFC1-6h and UFC2-4h selective layers.

The permeance, permeability and selectivity of the selective layer were calculated according to a previously established method (Fig. S15, ESI†)[38] and are listed in Table S1 and S2 (ESI†). Typically, for gas separation using polymeric membranes, permeance decreases as separation selectivity increases. Fig. 4b shows the relationship between CO_2 permeability and CO_2/N_2 selectivity of the UFC membrane selective layers compared to the data presented in a recent review[37] as well as those reported by Robeson[3]. The selective layer of UFC3-4h (P_{CO2} = 201 Barrer and $\alpha(CO_2/N_2)$ = 54, 1 Barrer = 10^{-10}·cm^3(STP)·cm·cm^{-2}·s^{-1}·cmHg^{-1}) demonstrates exceptional gas separation performance, approaching the most recent Robeson upper bound of conventional and state-of-the-art polymeric membranes for CO_2/N_2 separation. The selective layers of UFC3-4h with 25 *wt.*% XL3 generally exhibit improved CO_2/N_2 selectivity of > 40. In these UFC membranes, the grafting of P1 increases the CO_2 solubility and hence improves CO_2 permselectivity of the selective layer.

Extensive research has focused on developing different classes of membrane materials which display excellent gas separation performance to further reduce the cost of membrane technology. This includes inorganic zeolite-based membranes,[39,40] graphene-based membranes,[5] thermally rearranged (TR) membranes[1] and tetrazole-modified polymers of intrinsic microporosity (TZPIMs) membranes.[4] However, there remains a hurdle to economically form UFC membranes into spiral wound sheets or hollow fiber modules from these materials, due to their brittle nature. The low cost and ease of fabrication of the CAP-UFC membranes with PEG-based cross-linked selective layers; coupled with their demonstrated extremely high CO_2 permeance, improved CO_2 permeability and high CO_2/N_2 selectivity, makes these membranes very competitive for commercial UFC membrane module applications.

The mechanical properties, chemical resistance and time dependent stability of the UFC membranes were also measured. Generally, the mechanical strength of a composite membrane mainly relies on the mechanical property of its substrate. As shown in Figure S16a (ESI†), the PAN substrate presents an excellent mechanical strength (Young's modulus (E_{PAN}) = 894 MPa) and thus can provide significant mechanical strength to all UFC membranes. The cross-linked dense films using XL1 and XL2 also show high mechanical strength as revealed by their high Young's modulus values (E_{XL1} = 63.6 MPa and E_{XL2} = 105 MPa, Figure S16b-c, ESI†). As expected, the cross-linked film using XL3/P1 (1/3 wt. %) shows a lower Young's modulus ($E_{XL3/P1}$ = 0.67 MPa, Fig. S16d, ESI†) due to the addition of spacer P1, which significantly decreases the cross-linking density. The cross-linked UFC membranes present higher chemical resistance in comparison to a conventional composite membrane.[38] For example, the UFC3-4h membrane maintained its separation performance after exposure to a 30.6 mM H_2SO_4 solution for 12 hours. In contrast, a spin-coated composite membrane (Pebax/PEG-50%, Table S3, ESI†) lost >40 % of its selectivity under the same conditions. In addition, the UFC membranes also present excellent time dependent stability. After continuous exposure to a CO_2/N_2 mixed gas stream (10/90 v/v) for 7 days, the UFC membranes still maintained their separation performance (Table S4, ESI†). These results demonstrate enhanced mechanical stability and chemical resistance of the UFC membranes fabricated *via* the CAP cross-linking process.

For a conventional flat sheet composite membrane, the thickness of the selective layer is limited to greater than around 100 nm if defects are to be avoided. However, CAP ultra-thin films are grown from an initiator layer *via* a polymerization process (ARGET-ATRP) which obviates the need for perfectly flat substrate layers and overcomes the stringent conditions required for such thin films when scaling up. In addition, since selective layers of ~50 nm can be generated with much higher permeances, the membrane area required for effective carbon capture is vastly reduced.

In summary, UFC membranes for CO_2/N_2 separation were fabricated *via* a single-step CAP process on a microporous PAN substrate, which had been coated with a cross-linked PDMS initiator layer. The CAP-UFC membrane with the highest CO_2 permeance and with excellent CO_2/N_2 selectivity was found to form, by immersing the substrate into an aqueous solution containing catalyst and macrocross-linkers, for 4-6 hrs of polymerization. The performance of the UFC membranes successfully fell within the predicted economically viable target area for post-combustion CO_2 capture

membranes with a CO_2 permeance of 1,260 GPU and a CO_2/N_2 selectivity of > 40. This study opens up new avenues for CAP nanotechnology in the field of membrane separation processes.

Acknowledgements

This work was supported by the Australian Government through the CRC program (CO2CRC). We acknowledge the Australian Research Council under the Future Fellowship (FT110100411, G.G.Q.) and the Super Science Fellowship (FS110200025). Q. Fu acknowledges support from the University of Melbourne's 2013 Early Career Researcher Grant (Q. Fu). The authors are grateful to A/Prof. G. Wang for his help in synthesizing polymer precursor.

Notes and references

1 H. B. Park, C. H. Jung, Y. M. Lee, A. J. Hill, S. J. Pas, S. T. Mudie, E. V. Wagner, B. D. Freeman and D. J. Cookson, *Science*, 2007, **318**, 254-258.
2 N. Du, H. B. Park, M. M. Dal-Cina and M. D. Guiver, *Energy Environ. Sci.*, 2012, **5**, 7306-7322.
3 L. M. Robeson, *J. Membr. Sci.*, 2008, **320**, 390-400.
4 N. Du, H. B. Park, G. P. Robertson, M. M. Dal-Cin, T. Visser, L. Scoles and M. D. Guiver, *Nat. Mater.*, 2011, **10**, 372-375.
5 H. W. Kim, H. W. Yoon, S.-M. Yoon, B. M. Yoo, B. K. Ahn, Y. H. Cho, H. J. Shin, H. Yang, U. Paik, S. Kwon, J.-Y. Choi and H. B. Park, *Science*, 2013, **342**, 91-95.
6 T. C. Merkel, H. Lin, X. Wei and R. Baker, *J. Membr. Sci.*, 2010, **359**, 126-139.
7 H. Li, Z. Song, X. Zhang, Y. Huang, S. Li, Y. Mao, H. J. Ploehn, Y. Bao and M. Yu, *Science*, 2013, **342**, 95-98.
8 J. C. Jansen, M. G. Buonomenna, A. Figoli and E. Drioli, *Desalination* 2006, **193**, 58-65.
9 D. Li, T.-S. Chung and R. Wang, *J. Membr. Sci.*, 2004, **243**, 155-175.
10 P. Li, H. Z. Chen and T.-S. Chung, *J. Membr. Sci.*, 2013, **434**, 18-25.
11 T. K. Goh, S. N. Guntari, C. J. Ochs, A. Blencowe, D. Mertz, L. A. Connal, G. K. Such, G. G. Qiao and F. Caruso, *Small*, 2011, **7**, 2863-2867.
12 D. Mertz, C. J. Ochs, Z. Zhu, L. Lee, S. N. Guntari, G. K. Such, T. K. Goh, L. A. Connal, A. Blencowe, G. G. Qiao and F. Caruso, *Chem. Comm.*, 2011, **47**, 12601-12603.
13 E. H. H. Wong, S. N. Guntari, A. Blencowe, M. P. v. Koeverden, F. Caruso and G. G. Qiao, *ACS Macro Lett.*, 2012, **1**, 1020-1023.
14 S. N. Guntari, A. C. H. Khin, E. H. H. Wong, T. K. Goh, A. Blencowe, F. Caruso and G. G. Qiao, *Adv. Funct. Mater.*, 2013, **23**, 5159-5166.
15 E. Nam, J. Kim, S. N. Guntari, H. Seyler, Q. Fu, E. H. H. Wong, A. Blencowe, D. J. Jones, F. Caruso and G. G. Qiao, *Chem. Sci.*, 2014, **5**, 3374-3380.
16 Q. Wang, Z. Dong, Y. Du and J. F. Kennedy, *Carbohydr. Polym.*, 2007, **69**, 336-343.
17 J.-S. Wang and K. Matyjaszewski, *Macromolecules*, 1995, **28**, 7901-7910.
18 W. Jakubowski and K. Matyjaszewski, *Angew. Chem. Int. Ed.*, 2006, **45**, 4482-4486.
19 K. Matyjaszewski and N. V. Tsarevsky, *Nature Chem.*, 2009, **1**, 276-288.
20 W. Yave, A. Car, J. Wind and K.-V. Peinemann, *Nanotechnology*, 2010, **21**, 395301-395308.
21 C. E. Powell and G. G. Qiao, *J. Membr. Sci.*, 2006, **279**, 1-49.
22 H. Lin, T. Kai, B. D. Freeman, S. Kalakkunnath and D. S. Kalika, *Macromolecules*, 2005, **38**, 8381-8393.
23 H. Lin, E. V. Wagner, J. S. Swinnea, B. D. Freeman, S. J. Pas, A. J. Hill, S. Kalakkunnath and D. S. Kalika, *J. Membr. Sci.*, 2006, **276**, 145-161.
24 J. Xia, S. Liu and T.-S. Chung, *Macromolecules*, 2011, **44**, 7727-7736.
25 H. Azher, C. A.Scholes, G. W.Stevens and S. E.Kentish, *J. Membr. Sci.*, 2014, **459**, 104-113.
26 W. Yave, A. Car, S. S. Funari, S. P. Nunes and K.-V. Peinemann, *Macromolecules*, 2010, **43**, 326-333.
27 S. Duan, F. A. Chowdhury, T. Kai, S. Kazama and Y. Fujiok, *Desalination*, 2008, **234**, 278-285.
28 T. Brinkmann, C. Naderipour, J. Pohlmann, J. Wind, T. Wolff, E. Esche, D. Müller, G. Wozny and B. Hoting, *J. Membr. Sci.*, 2015, **489**, 237-247.
29 L. Bao and M. C. Trachtenberg, *J. Membr. Sci.*, 2006, **280**, 330-334.
30 A. Car, C. Stropnik, W. Yave and K.-V. Peinemann, *Sep. Purif. Technol.* , 2008, **62**, 110-117.
31 E. Toccia, A. Gugliuzza, L. D. Lorenzo, M. Macchione, G. D. Luca and E. Drioli, *J. Membr. Sci.*, 2008, **323**, 316-327.
32 A. Halim, Q. Fu, Q. Yong, P. A. Gurr, S. E. Kentish and G. G. Qiao, *J. Mater. Chem. A*, 2014, **2**, 4999-5009.
33 J. H. Kim and Y. M. Lee, *J. Membr. Sci.*, 2001, **193**, 209-225.
34 C. A. Scholes, J. Bacus, G. Q. Chen, W. X. Tao, G. Li, A. Qader, G. W. Stevens and S. E. Kentish, *J. Membr. Sci.*, 2012, **389**, 470-477.
35 A. Y. Alentiev, Shantarovich, T. C. Merkel, V. I. Bondar, B. D. Freeman and Y. P. Yampolskii, *Macromolecules*, 2002, **35**, 9513-9522.
36 H. B. Park and Y. M. Lee, *Adv. Mater.*, 2005, **17**, 477-483.
37 S. Kim and Y. M. Lee, *Curr. Opin. Chem. Eng.*, 2013, **2**, 238-244.
38 Q. Fu, A. Halim, J. Kim, J. M. P. Scofield, P. A. Gurr, S. E. Kentish and G. G. Qiao, *J. Mater. Chem. A*, 2013, **1**, 13769-13778.
39 S. Li and C. Q. Fan, *Ind. Eng. Chem. Res.*, 2010, **49**, 4399-4404.
40 J. C. White, P. K. Dutta, K. Shqau and H. Verweij, *Langmuir*, 2010, **26**, 10287-10293.

TOC

Defect-free and cross-linked ultra-thin (sub 100 nm) film composite membranes have been prepared. The membrane materials formed exhibited significantly high CO_2 permeances of over 1200 GPU as well as excellent CO_2/N_2 selectivity of over 40.